THE JOURNAL OF
PHYSICAL CHEMISTRY B

Article

pubs.acs.org/JPCB

Novel Guanidinium-Based Ionic Liquids for Highly Efficient SO_2 Capture

Xiaoxing Lu,[†] Jing Yu,[†] Jianzhou Wu,[†] Yongsheng Guo,*[,†] Hujun Xie,*[,‡] and Wenjun Fang*[,†]

[†]Department of Chemistry, Zhejiang University, Hangzhou 310027, PR China
[‡]Department of Applied Chemistry, Zhejiang Gongshang University, Hangzhou 310018, PR China

Ⓢ *Supporting Information*

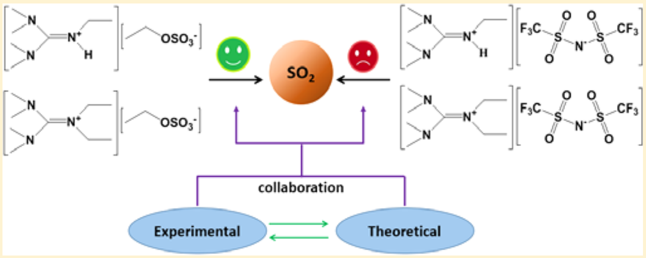

ABSTRACT: The application of ionic liquids (ILs) for acidic gas absorption has long been an interesting and challenging issue. In this work, the ethyl sulfate ($[C_2OSO_3]^-$) anion has been introduced into the structure of guanidinium-based ILs to form two novel low-cost ethyl sulfate ILs, namely 2-ethyl-1,1,3,3-tetramethylguanidinium ethyl sulfate ($[C_2{}^2(C_1)_2(C_1)_2{}^3gu][C_2OSO_3]$) and 2,2-diethyl-1,1,3,3-tetramethylguanidinium ethyl sulfate ($[(C_2)_2{}^2(C_1)_2(C_1)_2{}^3gu][C_2OSO_3]$). The ethyl sulfate ILs, together with 2-ethyl-1,1,3,3-tetramethylguanidinium bis(trifluoromethylsulfonyl)imide ($[C_2{}^2(C_1)_2(C_1)_2{}^3gu][NTf_2]$) and 2,2-diethyl-1,1,3,3-tetramethylguanidinium bis(trifluoromethylsulfonyl)imide ($[(C_2)_2{}^2(C_1)_2(C_1)_2{}^3gu][NTf_2]$), are employed to evaluate the SO_2 absorption and desorption performance. The recyclable ethyl sulfate ILs demonstrate high absorption capacities of SO_2. At a low pressure of 0.1 bar and at 20 °C, 0.71 and 1.08 mol SO_2 per mole of IL can be captured by $[C_2{}^2(C_1)_2(C_1)_2{}^3gu][C_2OSO_3]$ and $[(C_2)_2{}^2(C_1)_2(C_1)_2{}^3gu][C_2OSO_3]$, respectively. The absorption enthalpy for SO_2 absorption with $[C_2{}^2(C_1)_2(C_1)_2{}^3gu][C_2OSO_3]$ and $[(C_2)_2{}^2(C_1)_2(C_1)_2{}^3gu][C_2OSO_3]$ are −3.98 and −3.43 kcal mol^{-1}, respectively. While those by $[C_2{}^2(C_1)_2(C_1)_2{}^3gu][NTf_2]$ and $[(C_2)_2{}^2(C_1)_2(C_1)_2{}^3gu][NTf_2]$ turn out to be only 0.17 and 0.24 mol SO_2 per mole of IL under the same conditions. It can be concluded that the guanidinium ethyl sulfate ILs show good performance for SO_2 capture. Quantum chemistry calculations reveal nonbonded weak interactions between the ILs and SO_2. The anionic moieties of the ILs play an important role in SO_2 capture on the basis of the consistently experimental and computational results.

■ INTRODUCTION

The capture of SO_2, one of the most hazardous sources of air pollution, has long been an important issue because it is concerned about both the environment and human health. Many kinds of methods and techniques have been developed to deal with the capture of SO_2. The main disadvantage of the most widely applied absorption technique, that is limestone scrubbing,[1,2] is the significant secondary pollution caused by the CO_2 emission and the large amount of wastewater.

For the past few years, methods and techniques related to the ionic liquids (ILs) have drawn intensive attention in the processes of gas absorption for hazardous acidic gases, such as CO_2,[2−9] SO_2,[10−16] and NO_x.[17,18] This kind of process has been developed on the basis of the appealing properties of various ILs, such as the mostly studied imidazolium-based ILs. The achievements made by researchers have proved that ILs are promising materials in the application of hazardous gas absorption. However, the costs of operations involving ILs are still high. For example, from the aspect of synthesis of ILs, a two-step synthesis procedure is usually required for the preparation of many ILs, which is supposed to be time-consuming and high-cost. The imidazolium-based ILs, such as 1-ethyl-3-methylimidazolium thiocyanate ($[C_2C_1im][SCN]$),[10] 1-butyl-3-methylimidazolium lactate ($[C_4C_1im][(OH)^2C_2CO_2]$),[14] and 1-butyl-3-methylimidazolium tetrafluoroborate ($[C_4C_1im][BF_4]$),[15,19] with satisfactory results of SO_2 absorption, usually come from the traditional two-step synthesis. Nevertheless, fair amounts of the common ILs like $[C_4C_1im][BF_4]$ have become commercial products for various applications. It may help alleviate the main cost problem, but the preparations are still not economical enough.

Except for imidazolium-based ILs, there are other kinds of ILs, such as a variety of guanidinium-based ILs with different anions, which also demonstrate good performance for the absorption of SO_2. The guanidinium-based ILs are found to be very useful and efficient in many scientific fields involving catalytic process,[20,21] dissolution or extraction,[22−24] and gas absorption.[12,13,25−28] The studies of 1,1,3,3-tetramethylguanidinium lactate ([TMG][Lac]) opened up the possibility for deep and wide investigations of guanidinium-based ILs. For instance, it has been proven that [TMG][Lac] has the ability to absorb SO_2 and CO_2,[12,29,30] while the main defect is its poor regeneration behavior[27] along with its extremely high dynamic viscosity (>10^4 mPa s^{-1}) under ambient conditions.[31] Huang et

Received: January 28, 2015
Revised: April 12, 2015

Scheme 1. Synthetic Strategies of Guanidinium-Based Ionic Liquids

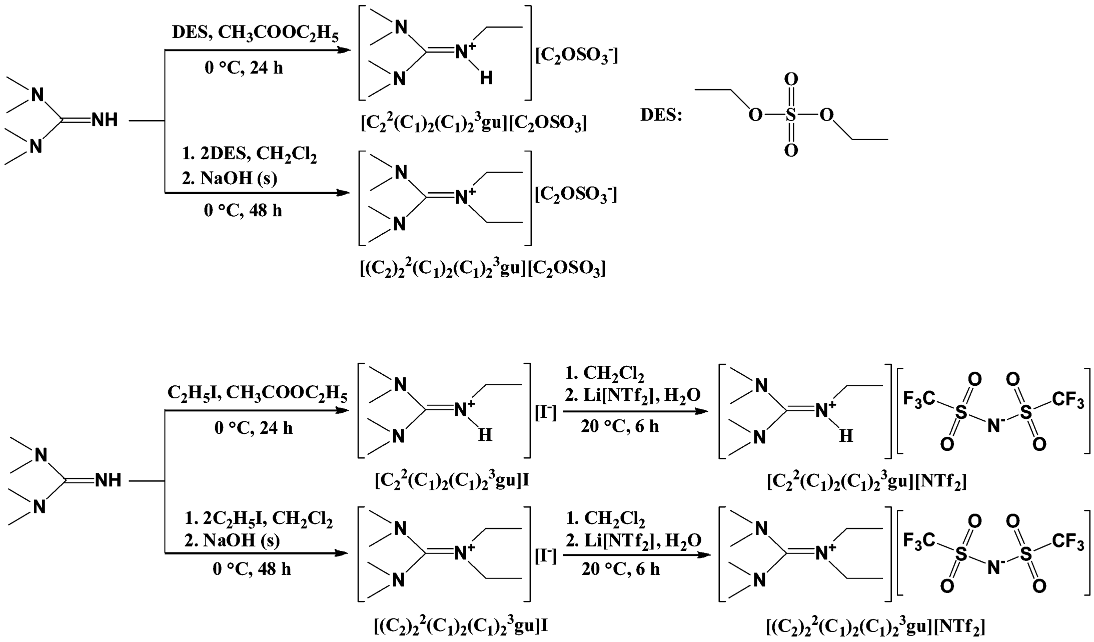

al.[13,26] reported the results of SO_2 capture with a number of tuning guanidinium-based ILs possessing the $[NTf_2]^-$ anion, and also provided new approaches to the syntheses of multisubstituted guanidinium-based ILs. About 0.08 mol fraction of SO_2 was captured at a low partial pressure of 0.1 bar and at 20 °C by the $[NTf_2]$-based ILs. Hence, it is very important to discover novel ILs at a low cost, which are suitable to capture acidic gases like SO_2 under the particular circumstances.

In previous work, we employed [TMG][Lac] to the extractive desulfurization process of hydrocarbon fuels, along with three piperazinium-based ILs. It is found that [TMG][Lac] has the highest extractive efficiency and selectivity.[24] As a continuation of the previous efforts, two novel guanidinium-based ILs, 2-ethyl-1,1,3,3-tetramethylguanidinium ethyl sulfate ($[C_2{}^2(C_1)_2(C_1)_2{}^3gu][C_2OSO_3]$) and 2,2-diethyl-1,1,3,3-tetramethylguanidinium ethyl sulfate ($[(C_2)_2{}^2(C_1)_2(C_1)_2{}^3gu][C_2OSO_3]$), have been designed and employed to capture SO_2 in the present work. When guanidinium-based ILs with dicyanamide, thiocyanide, and tetrafluoroboric anions appear hygroscopic solids, the ethyl sulfate anion that comes from the cheap commercial product, diethyl sulfate, is introduced with fine properties. The absorption/desorption performance for the ILs was demonstrated under different conditions. Two ILs with the same cations with those of the ethyl sulfate ILs, $[C_2{}^2(C_1)_2(C_1)_2{}^3gu][NTf_2]$ and $[(C_2)_2{}^2(C_1)_2(C_1)_2{}^3gu][NTf_2]$, were investigated to show a comparison of the effect of anions on absorption performance. While another two ethyl sulfate ILs, 1-ethyl-3-methylimidazolium ethyl sulfate ($[C_2C_1im][C_2OSO_3]$) and 1-ethyl-3-methylpyridinium ethyl sulfate ($[C_2py][C_2OSO_3]$), were also employed to demonstrate a comparison of the effect of cations. The interactions between ILs and SO_2 were further studied from a computational perspective.

EXPERIMENTAL SECTION

Materials. 1,1,3,3-Tetramethylguanidine (Aldrich, ≥ 0.990 in mass fraction), diethyl sulfate (Aldrich, ≥ 0.980), sodium hydroxide (Sigma−Aldrich, ≥ 0.980), bis(trifluoromethylsulfonyl)imide lithium ($Li[NTf_2]$, Aldrich, 0.9995 trace metals basis), iodoethane (Sigma−Aldrich, ≥ 0.990) dichloromethane (Sigma−Aldrich, ≥ 0.998) and ethyl acetate (Sigma−Aldrich, ≥ 0.998) were used without further purification. A Millipore Q3 system was applied to produce ultrapure water.

SO_2 (≥0.999) gas and N_2 gas (≥0.999) were purchased from Hangzhou Jingong Special Gas Co. Ltd., PRC.

The studied ILs, $[C_2{}^2(C_1)_2(C_1)_2{}^3gu][C_2OSO_3]$, $[(C_2)_2{}^2(C_1)_2(C_1)_2{}^3gu][C_2OSO_3]$, $[C_2{}^2(C_1)_2(C_1)_2{}^3gu][NTf_2]$ and $[(C_2)_2{}^2(C_1)_2(C_1)_2{}^3gu][NTf_2]$, were synthesized in the laboratory.

Preparation and Characterization of the ILs. The tetramethylguanidinium ethyl sulfate and bis(trifluoromethylsulfonyl)imide ILs were synthesized according to Scheme 1.

$[C_2{}^2(C_1)_2(C_1)_2{}^3gu][C_2OSO_3]$ and $[(C_2)_2{}^2(C_1)_2(C_1)_2{}^3gu][C_2OSO_3]$ were prepared by a one-pot reaction, while $[C_2{}^2(C_1)_2(C_1)_2{}^3gu][NTf_2]$ and $[(C_2)_2{}^2(C_1)_2(C_1)_2{}^3gu][NTf_2]$ were prepared by the two-step methods.[13,32] The detailed information for the preparation of the ILs is presented in the Supporting Information. The water content in the ILs was determined using a coulometer (Mettler Toledo, C20) by a Karl Fischer titration. The water mass fraction was less than 200 ppm.

Characterizations of the ILs with ^1H and ^{13}C NMR spectra were carried out on a Bruker AVANCE III 500 MHz NMR spectrometer using $CDCl_3$ as solvent and tetramethylsilane as the internal standard. The results are shown in Figures S-1 to S-8 in the Supporting Information.

The densities of the guanidinium-based ILs were measured with a densimeter (Anton Paar DMA, 5000 M), which was calibrated with ultrapure water and dry air. The results are summarized in Table S-1. The uncertainty is 0.01 °C for the temperature and 3×10^{-5} g cm^{-3} for the density.

1-Ethyl-3-methylimidazolium ethyl sulfate ($[C_2C_1im][C_2OSO_3]$) and 1-ethyl-3-methylpyridinium ethyl sulfate

($[C_2py][C_2OSO_3]$) were prepared according to the same procedures with those of $[C_2{}^2(C_1)_2(C_1)_2{}^3gu][C_2OSO_3]$ to show a comparison with the guanidinium-based ILs on gas capture.

Thermal Stability of the ILs. Characterizations of the thermal stability of ILs were carried out on a thermal gravimetric analyzer (TA Instruments, Q50) under a nitrogen atmosphere. An approximate amount of 5.0 mg of IL and a ceramic crucible were applied for scanning at the heating rate of 5 °C min^{-1} from room temperature to 500 °C.

SO_2 Absorption/Desorption. The apparatus for SO_2 absorption in this work is schematically illustrated in Figure 1.

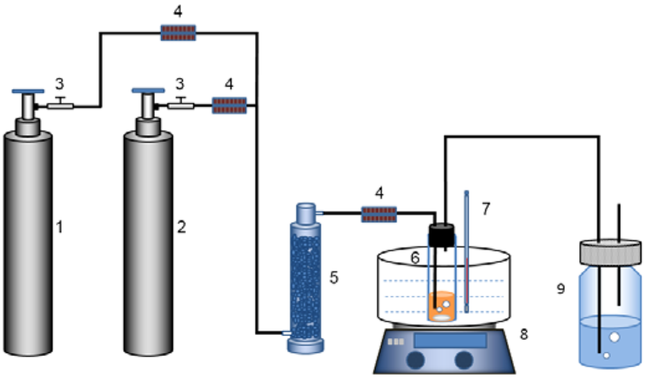

Figure 1. Apparatus applied for SO_2 absorption: 1, N_2 gas cylinder; 2, SO_2 gas cylinder; 3, valve; 4, gas flowmeter; 5, drying tower; 6, IL-containing quartz tube; 7, thermometer; 8, temperature controller; 9, tail gas absorber.

A certain amount of IL (*c.a.* 3.0 g) was loaded to a quartz tube (100 mm in height and 30 mm in diameter) immersed in a water bath (IKA, RCT basic). The diameter of the nozzle of the gas inlet is 4.0 mm. The quartz tube was previously heated at 100 °C before each experiment under vacuum. The temperature is controlled with an accuracy of 0.1 °C. Then, pure SO_2 gas or mixed gas consisting of SO_2 and N_2 was introduced into IL by bubbling at the flow rate of 60 mL min^{-1}. The flow rate of gas was controlled by a rotometer (Changzhou Shuanghuan Thermo-technical Instrument Co., Ltd., LZB-3WB). Pretests of N_2 absorption with ILs were carried out and it is confirmed that the solubility of N_2 in the ILs is negligible (<0.0001 g). Therefore, the content of absorbed SO_2 can be determined by mass (Mettler Toledo, AL204) with an uncertainty of 0.0001 g. The absorption equilibrium was supposed to be achieved when the measured mass of the tube containing IL remained unchanged.

As soon as the absorption equilibrium was reached, SO_2 in the IL was desorbed by heating up to 50 °C with the bubbling of N_2 gas at the pressure of 1 bar into IL at the flow rate of 60 mL min^{-1}, and the mass changes were recorded periodically. Desorption tests under vacuum (<20 Pa, 25 °C) were also carried out. Each test for absorption/desorption was conducted at least 2 times.

The uncertainties for the temperature (T), pressure (p), gas flow (Q), and time (t) are $u(T) = 0.1$ °C, $u(p) = 0.2$ kPa, $u(Q) = 3$ mL min^{-1}, and $u(t) = 1$ s. The uncertainty for the amount of SO_2 in the ILs (x, mole SO_2 per mole IL) is $u(x) = 0.04x$.

FT-IR Characterization. A Nicolet 470 spectrophotometer (Thermo Electron Co.) with the OMIC software was employed to record FT-IR spectra for the ILs before and after SO_2 capture.

Computational Methods. Quantum chemistry calculations were carried out by density functional theory (DFT) at the B3LYP level of theory,[33−35] in combination with the 6-311+G(d,p) basis set to optimize all species. Frequency calculations were also performed to obtain the zero point energy (ZPE) and identify the stationary points as minima. Possible isomers for different complexes of IL−$n(SO_2)$ (n = 0−4) have been evaluated, and the most stable geometries are presented. All calculations were performed with the Gaussian 09 software package.[36]

■ RESULTS AND DISCUSSION

Enormous efforts in experimental and computational have been done in order to study the capture of SO_2 by room temperature ionic liquids (RTILs). In general, it is supposed that the SO_2 absorption is dominated by the interactions between the anion of the IL and SO_2 molecule.[26,37,38] However, there is a main consideration that a high basicity of the anionic moiety may consequently block the regeneration of IL because of the enhanced interactions between the absorbent and SO_2, leading to the requirement of stringent conditions for gas desorption. Therefore, the mild functional groups or atoms such as ether groups or oxygen atoms which form interactions with SO_2 with suitable strength can be introduced.[27,39] The nonbonded interactions generated between absorbent and SO_2 can assist the absorption and facilitate the desorption.

Thermal Stabilities. To check whether the ILs are suitable for SO_2 capture, evaluations of their thermal stabilities were carried out. The thermogravimetric analysis (TGA) traces are shown in Figure 2. For $[C_2{}^2(C_1)_2(C_1)_2{}^3gu][C_2OSO_3]$, the IL shows a gradual weight loss for no more than 2.5% from 40 °C up to about 110 °C, which comes from the continuous decomposition of the ethyl sulfate anion to sulfate or hydrogensulfate rather than the decomposition of the ethyl group in the cation. The speculation is confirmed by ^1H NMR spectrum (Figure S-9) after heating the IL to 110 °C. This weight loss increases to 10.5% around 220 °C representing a loss of approximate 28 or 29 g mol^{-1}. This kind of thermal behavior is similar to those of imidazolium ethyl sulfate ILs reported in the literature.[40] Meanwhile, the weight loss of $[(C_2)_2{}^2(C_1)_2(C_1)_2{}^3gu][C_2OSO_3]$ is 10.0% at 250 °C which similarly represent the complete decomposition of ethyl sulfate

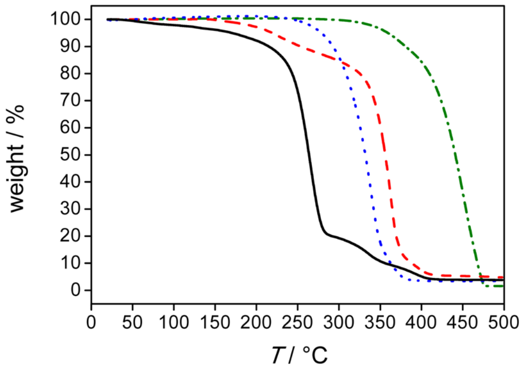

Figure 2. TGA curves of the ILs: solid line, $[C_2{}^2(C_1)_2(C_1)_2{}^3gu][C_2OSO_3]$; dashed line, $[(C_2)_2{}^2(C_1)_2(C_1)_2{}^3gu][C_2OSO_3]$; dotted line, $[C_2{}^2(C_1)_2(C_1)_2{}^3gu][NTf_2]$; dash−dotted line, $[(C_2)_2{}^2(C_1)_2(C_1)_2{}^3gu][NTf_2]$.

anion. Interestingly, another weight loss of 10.0% at 325 °C is followed. It can be ascribed to the departure of one ethyl group in the guanidinium cation. The decomposition curves of $[NTf_2]$-based ILs show much higher thermal stabilities compared with those of $[C_2OSO_3]$-based ILs, as a result of a more stable anion. The hexa-substituted ones are more stable to heat relative to the penta-substituted ones because of the better symmetry of the cation. In conclusion, these ILs are supposed to have adequate thermal stabilities.

SO_2 Absorption with Ionic Liquids. Absorption experiments at an atmospheric pressure (p = 1 bar) and at 20 °C were done with the results shown in Figure 3.

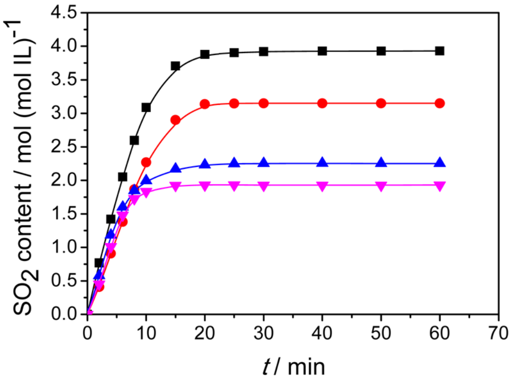

Figure 3. SO_2 absorption with different ILs at an atmospheric pressure (1 bar) and 20 °C: ■, $[(C_2)_2{}^2(C_1)_2(C_1)_2{}^3gu][C_2OSO_3]$; ●, $[C_2{}^2(C_1)_2(C_1)_2{}^3gu][C_2OSO_3]$; ▲, $[(C_2)_2{}^2(C_1)_2(C_1)_2{}^3gu][NTf_2]$; ▼, $[C_2{}^2(C_1)_2(C_1)_2{}^3gu][NTf_2]$.

It is observed that the maximum absorption capacity is achieved in 20 min, and the absorption performance is in the order of $[(C_2)_2{}^2(C_1)_2(C_1)_2{}^3gu][C_2OSO_3]$ > $[C_2{}^2(C_1)_2(C_1)_2{}^3gu][C_2OSO_3]$ > $[(C_2)_2{}^2(C_1)_2(C_1)_2{}^3gu][NTf_2]$ > $[C_2{}^2(C_1)_2(C_1)_2{}^3gu][NTf_2]$. $[(C_2)_2{}^2(C_1)_2(C_1)_2{}^3gu][C_2OSO_3]$ absorbs 3.93 mol SO_2 per mole of IL, and the two $[NTf_2]$-based ILs have the capacities of about 2 mol SO_2 per mole of IL. Both ILs with hexa-substituted guanidinium cations show larger capacities.

Moreover, it is found that the guanidinium ethyl sulfate ILs have higher absorption capacities compared with $[C_2C_1im][C_2OSO_3]$ and $[C_2py][C_2OSO_3]$ at 20 °C and 1 bar, which show the capacities of 2.60 and 2.85 mol SO_2 per mole of IL respectively. In literature, at 16 °C and 1 bar, about 2 mol SO_2 per mole of IL can be absorbed by $[C_2C_1im][C_2OSO_3]$.[41,42] These observations demonstrate that the ethyl sulfate ILs with guanidinium cation are more efficient for the absorption of SO_2.

Subsequently, in order to obtain more practical results of the flue gas desulfurization with the ILs, a gas mixture of SO_2/N_2 with SO_2 content of 10% by volume was employed instead of the pure SO_2 gas. The SO_2 absorption performance of ethyl sulfate ILs at different temperatures of 20, 30, and 40 °C is evaluated to calculate the heat of absorption. The results are shown in Figure 4.

The rise of temperature from 20 to 40 °C results in a remarkable drop of SO_2 capacity. It is observed that 0.71 and 1.08 mol SO_2 per mole of IL have been captured at 20 °C by $[C_2{}^2(C_1)_2(C_1)_2{}^3gu][C_2OSO_3]$ and $[(C_2)_2{}^2(C_1)_2(C_1)_2{}^3gu][C_2OSO_3]$, respectively. The absorption capacities drop to 0.36 and 0.55 mol SO_2 per mole IL at 40 °C. The SO_2 capture is reduced and the required time to reach equilibrium is increased significantly compared with those for atmospheric SO_2. Nevertheless, the ethyl sulfate ILs performed well in the simulation of practical SO_2 absorption process.

The absorption equilibrium can be expressed as

$$SO_2(\text{gas}) \rightleftharpoons SO_2(\text{IL}) \tag{1}$$

Henry's law is used to describe the behavior of gas absorption at 0.1 bar of SO_2, and we have the following equation:

$$K = \frac{x}{p} \tag{2}$$

where K is Henry's constant, x represents the mole fraction of SO_2 in the IL phase, and p represents the partial pressure of SO_2 in the gas phase. The heat of gas absorption from phase-equilibrium data can be calculated according to the following equation:[43]

$$\frac{d[\ln K]}{dT} = \frac{\Delta H_{abs}}{RT^2} \tag{3}$$

where ΔH_{abs} represents the absorption enthalpy. The calculated results of K and ΔH_{abs} are summarized in Table 1.

The absorption enthalpies for SO_2 absorption with $[C_2{}^2(C_1)_2(C_1)_2{}^3gu][C_2OSO_3]$ and $[(C_2)_2{}^2(C_1)_2(C_1)_2{}^3gu][C_2OSO_3]$ are −3.98 and −3.43 kcal mol^{-1}, respectively. Although these values are slightly higher relative to those for SO_2 absorption with N-functionalized imidazole at 25 °C and

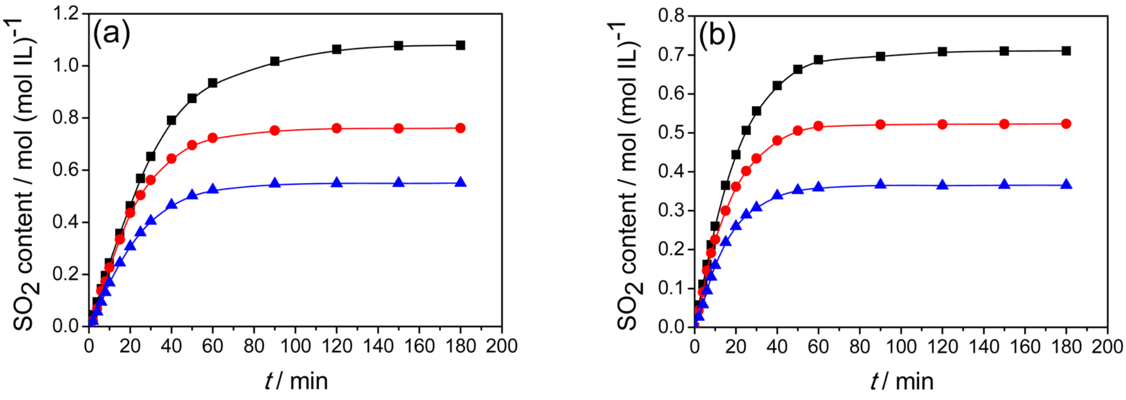

Figure 4. SO_2 absorption with (a) $[(C_2)_2{}^2(C_1)_2(C_1)_2{}^3gu][C_2OSO_3]$ and (b) $[C_2{}^2(C_1)_2(C_1)_2{}^3gu][C_2OSO_3]$ at a pressure of SO_2 of 0.1 bar and different temperatures: ■, 20 °C; ●, 30 °C; ▲, 40 °C.

DOI: 10.1021/acs.jpcb.5b00921

Table 1. Henry's Constant (K) and Absorption Enthalpy (ΔH_{abs}) in the Process of SO_2 Absorption with Guanidinium Ethyl Sulfate ILs at 0.1 bar

	$[C_2{}^2(C_1)_2(C_1)_2{}^3gu][C_2OSO_3]$		$[(C_2)_2{}^2(C_1)_2(C_1)_2{}^3gu][C_2OSO_3]$	
T/°C	K/bar^{-1}	ΔH_{abs}/kcal mol^{-1}	K/bar^{-1}	ΔH_{abs}/kcal mol^{-1}
20	4.15		5.19	
30	3.42	−3.98	4.32	−3.43
40	2.67		3.55	

144.8 kPa,[44] they are still small to indicate a possible physical absorption process for the guanidinium-based ILs.

On the other hand, only 0.17 and 0.24 mol SO_2 per mole of IL is captured at 20 °C with $[C_2{}^2(C_1)_2(C_1)_2{}^3gu][NTf_2]$ and $[(C_2)_2{}^2(C_1)_2(C_1)_2{}^3gu][NTf_2]$, respectively, as shown in Figure 5. The absorbed amounts of SO_2 for $[NTf_2]$-based ILs is approximate 1/10 of those for the atmospheric SO_2 at 20 °C, showing a remarkable drop.

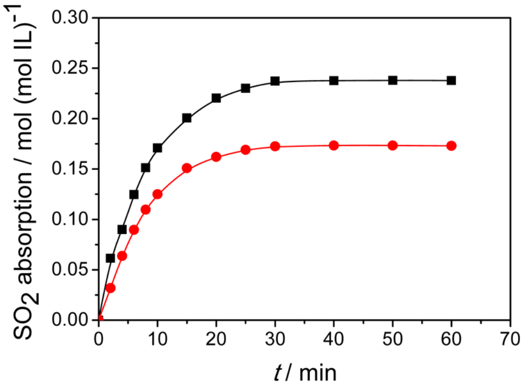

Figure 5. SO_2 absorption with the $[NTf_2]$-based ILs at a SO_2 pressure of 0.1 bar and 20 °C: ■, $[(C_2)_2{}^2(C_1)_2(C_1)_2{}^3gu][NTf_2]$; ●, $[C_2{}^2(C_1)_2(C_1)_2{}^3gu][NTf_2]$.

Regeneration of the Ionic Liquids. As the ethyl sulfate ILs exhibited good absorption ability, we examined the regeneration ability of the ILs. Typical cycles of absorption/desorption of SO_2 with the ethyl sulfate ILs are depicted in Figure 6. It is observed that the absorbed SO_2 is completely removed after the desorption process.

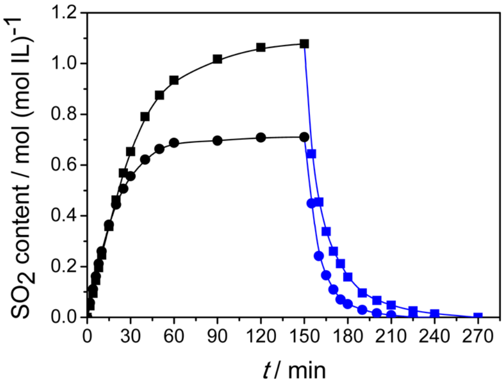

Figure 6. Typical cycle of absorption/desorption of SO_2 with ethyl sulfate ILs. SO_2 is absorbed at a pressure of 0.1 bar mixed with N_2 and at 20 °C, and desorbed at 50 °C with the atmospheric N_2 bubbling: ■, $[(C_2)_2{}^2(C_1)_2(C_1)_2{}^3gu][C_2OSO_3]$; ●, $[C_2{}^2(C_1)_2(C_1)_2{}^3gu][C_2OSO_3]$.

It should be mentioned that a relatively low temperature of 50 °C was applied in the desorption process, because there is a consideration of the fair thermal stability of $[C_2{}^2(C_1)_2(C_1)_2{}^3gu][C_2OSO_3]$ on the basis of the TGA results previously described. Thus, desorption of SO_2 was achieved under vacuum at the room temperature in lieu of desorption by heating with N_2 bubbling, which turned out to be very suitable for these ILs. Successive multicycles of absorption/desorption of SO_2 with $[C_2{}^2(C_1)_2(C_1)_2{}^3gu][C_2OSO_3]$ and $[(C_2)_2{}^2(C_1)_2(C_1)_2{}^3gu][C_2OSO_3]$ are also displayed in Figure 7. The ILs were dried again after desorption. Ten successful consecutive absorption/desorption cycles indicate the ILs can be well regenerated without loss in absorption capability.

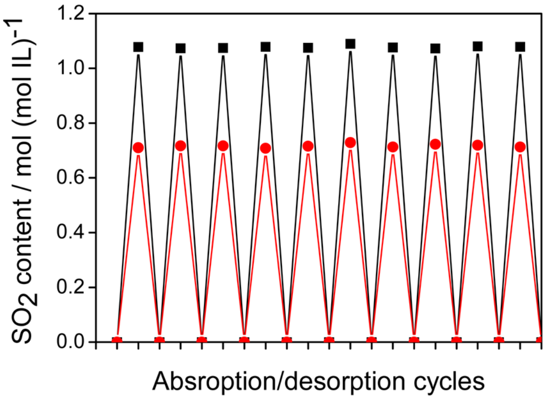

Figure 7. Successive cycles of SO_2 absorption/desorption with the ethyl sulfate ILs. SO_2 is absorbed at a pressure of 0.1 bar mixed with N_2 and at 20 °C, and desorbed at <20 Pa and 25 °C: ■, $[(C_2)_2{}^2(C_1)_2(C_1)_2{}^3gu][C_2OSO_3]$; ●, $[C_2{}^2(C_1)_2(C_1)_2{}^3gu][C_2OSO_3]$.

In addition, the highest water content in the ILs was determined to be about 800 ppmw for $[(C_2)_2{}^2(C_1)_2(C_1)_2{}^3gu]$-$[C_2OSO_3]$ after each SO_2 absorption process among 10 consecutive regeneration cycles, when the absorption capacity increased to *ca.* 1.10 mol SO_2 per mole of IL, indicating that the change of water content in the ILs has a slight influence on the performance of SO_2 capture. Nevertheless, water is not added to the ILs to absorb SO_2 as it hydrolyzes SO_2 severely. The cost for regeneration of ILs is elevated as well when water is introduced.

Geometries of Ionic Liquids. With the experimental data in hand, we simulated the molecular structures of the guanidinium-based ILs by quantum chemistry calculations. The optimized molecular structures of the ILs are shown in Figure 8, along with those of ILs containing the $[NTf_2]^-$ anion.

It is found that the hydrogen-bonding interaction through N−H···O with the spans of 1.75 or 1.82 Å is presented in both penta-substituted guanidinium-based ILs (Figure 8, parts a and c), and it does not exist in the hexa-substituted ones (Figure 8, parts b and d). The particular spatial distribution of N−H···O leads to a quite strong hydrogen-bonding interaction between the cation and anion, and the interaction enthalpy (ΔH) has been obviously shifted by ∼7 kcal mol^{-1} from −78.1 to −85.6 kcal mol^{-1} or from −69.9 to −76.6 kcal mol^{-1}. The hydrogen-bonding interaction of N−H···O between cation and anion that only exists in the ILs with penta-substituted guanidinium cations accounts for the weakening of the interactions between IL and SO_2 molecules.

Interactions between the ILs and SO_2 via DFT Calculations. DFT calculations allow the analysis of the

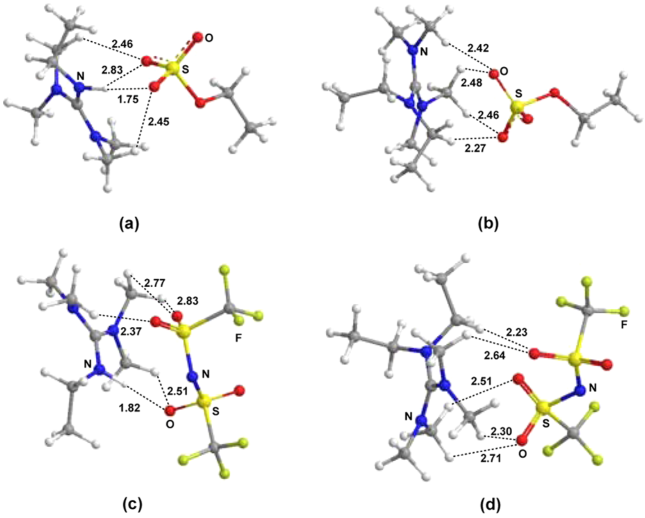

Figure 8. Optimized structures of the ILs showing interactions between cation and anion moieties (bond lengths are shown in Å): (a) $[C_2{}^2(C_1)_2(C_1)_2{}^3gu][C_2OSO_3]$ (ΔH = −85.6 kcal mol^{-1}); (b) $[(C_2)_2{}^2(C_1)_2(C_1)_2{}^3gu][C_2OSO_3]$ (ΔH = −78.1 kcal mol^{-1}); (c) $[C_2{}^2(C_1)_2(C_1)_2{}^3gu][NTf_2]$ (ΔH = −76.6 kcal mol^{-1}); (d) $[(C_2)_2{}^2(C_1)_2(C_1)_2{}^3gu][NTf_2]$ (ΔH = −69.9 kcal mol^{-1}).

interactions between the ILs and SO_2. Previous quantum chemistry calculations[19,30] have clearly revealed the interaction patterns of [TMG][Lac] with CO_2 or SO_2 successfully. Herein, we adopted this method to get deep insights into the interactions between the guanidinium-based ILs and SO_2. Structure optimizations for ILs and SO_2 were achieved and the results are displayed in Figures 9−12, and the interaction enthalpies are listed in Table 2.

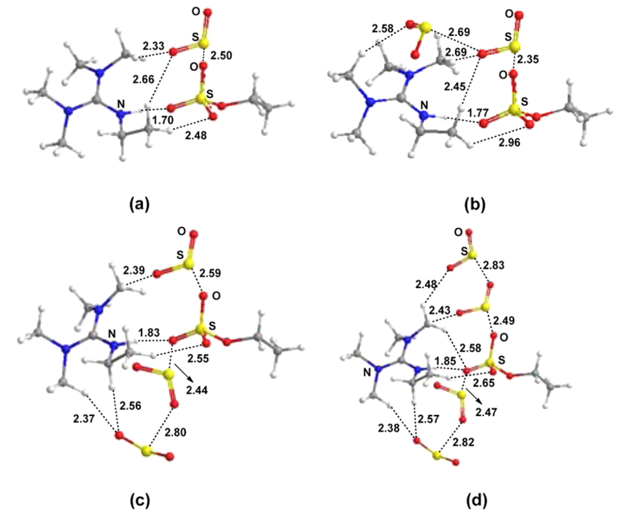

Figure 9. Optimized structures of $[C_2{}^2(C_1)_2(C_1)_2{}^3gu][C_2OSO_3]$ with SO_2 showing interactions between IL moieties and SO_2 (bond lengths are shown in Å): (a), IL + SO_2; (b), IL + $2SO_2$; (c), IL + $3SO_2$; (d), IL + $4SO_2$.

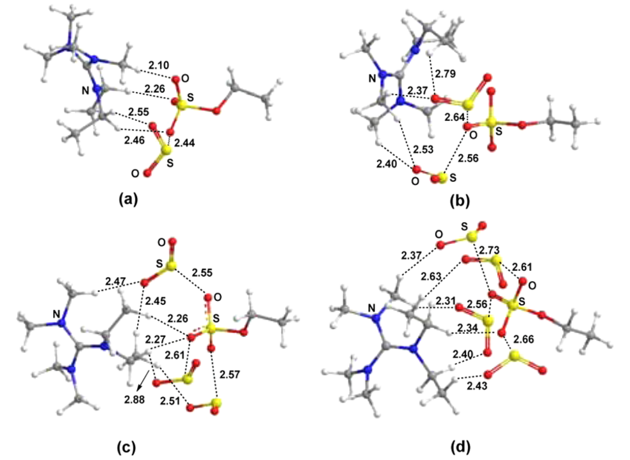

Figure 10. Optimized structures of $[(C_2)_2{}^2(C_1)_2(C_1)_2{}^3gu][C_2OSO_3]$ with SO_2 showing interactions between IL moieties and SO_2 (bond lengths are shown in Å): (a), IL + SO_2; (b), IL + $2SO_2$; (c), IL + $3SO_2$; (d), IL + $4SO_2$.

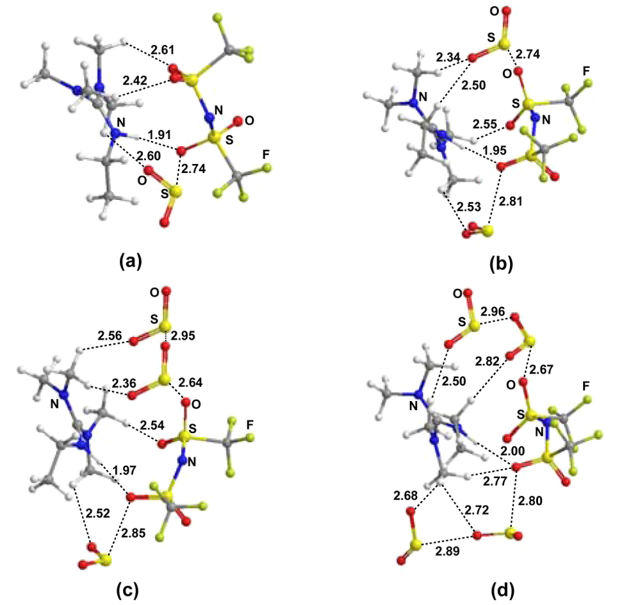

Figure 11. Optimized structures of $[C_2{}^2(C_1)_2(C_1)_2{}^3gu][NTf_2]$ with SO_2 showing interactions between IL moieties and SO_2 (bond lengths are shown in Å): (a), IL + SO_2; (b), IL + $2SO_2$; (c), IL + $3SO_2$; (d), IL + $4SO_2$.

The enthalpy increments for the addition of SO_2 molecules to the ILs reveal that the more the SO_2, the larger the enthalpy is. As reported in Table 2, the ΔH values are related to the absorption ability and the absorption performance of the ILs seems to follow the order: $[C_2{}^2(C_1)_2(C_1)_2{}^3gu][C_2OSO_3]$ > $[(C_2)_2{}^2(C_1)_2(C_1)_2{}^3gu][C_2OSO_3]$ > $[(C_2)_2{}^2(C_1)_2(C_1)_2{}^3gu][NTf_2]$ ≈ $[C_2{}^2(C_1)_2(C_1)_2{}^3gu][NTf_2]$. In general, the calculations are in agreement with the experimental results. Among the studied systems for four ILs, ΔH increases the most for $[(C_2)_2{}^2(C_1)_2(C_1)_2{}^3gu][C_2OSO_3]$ from 6.0 kcal mol^{-1} (IL + $1SO_2$) to 27.8 kcal mol^{-1} (IL + $4SO_2$), and the ΔH increment with each addition of one SO_2 molecule is generally the largest. The intrinsic hydrogen-bonding interaction in the pentasubstituted guanidinium ILs severely prevents the interaction between the IL and SO_2, and the SO_2 capability is observed lower relative to the corresponding hexa-substituted ones. Hence, gas capture performance is better for $[(C_2)_2{}^2(C_1)_2(C_1)_2{}^3gu][C_2OSO_3]$ than $[C_2{}^2(C_1)_2(C_1)_2{}^3gu][C_2OSO_3]$, which is in accordance with experimental results. Additionally, it is noted that the strength of H-bonding interaction is gradually weakening with the increasing SO_2 amount, as the distance of N−H···O becomes slightly longer

DOI: 10.1021/acs.jpcb.5b00921

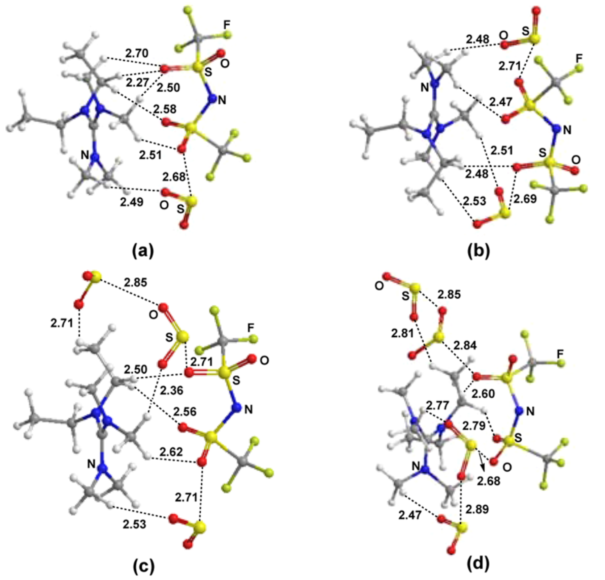

Figure 12. Optimized structures of $[(C_2)_2{}^2(C_1)_2(C_1)_2{}^3gu][NTf_2]$ with SO_2 showing interactions between IL moieties and SO_2 (bond lengths are shown in Å): (a), IL + SO_2; (b), IL + $2SO_2$; (c), IL + $3SO_2$; (d), IL + $4SO_2$.

from 1.70 to 1.85 Å for $[C_2{}^2(C_1)_2(C_1)_2{}^3gu][C_2OSO_3]$ and from 1.91 to 2.00 Å for $[C_2{}^2(C_1)_2(C_1)_2{}^3gu][NTf_2]$, indicating the probable competitive relation between anion−cation and IL−SO_2 interactions.

Furthermore, we also noted that the SO_2 molecules interact not only with the IL moieties, but also with other SO_2 molecules through the O═S···O weak interactions with a spans of 2−3 Å. The oxygen atoms in a SO_2 molecule becomes more nucleophilic when the SO_2 molecule has been bonded to the ethysulfate anion.[27] This kind of interaction offers great help to capture more SO_2, that once one SO_2 molecule is captured, more SO_2 molecules aggregate later.

Referring to calculated results, we conclude three types of interactions among the ILs and SO_2: interactions between the cation and SO_2 through C−H···O, the packing effect among different SO_2 molecules, and interactions between the anion and SO_2 through S═O···S. Combined with the experimental results, it is considered that the third kind of interactions play the predominant role in SO_2 absorption with the ILs. The sulfate moiety of the ethyl sulfate anion has three oxygen atoms closer to each other relative to the $[NTf_2]^-$ anion, facing toward the N^+ atom in the cationic moiety. The bridge structures of H···O═S···O representing cation−SO_2−anion interactions for the ethyl sulfate ILs are easily generated and may facilitate the capture of SO_2 even at a low pressure.

Likewise, Costa et al.[45] calculated the interactions of a number of ILs with CO_2, H_2S, and SO_2, including imidazolium NTf_2 ILs. They evaluated the CO_2 solubility in $[C_2C_1im]$-$[NTf_2]$ from the a microscopic point of view.[46] Free volume, which is rather popular in previous theoretical and experimental practices,[47−50] has been discussed to relate with the gas solubility, while relatively weak correlation was found.[46,47] In this work, the ILs with the $[NTf_2]^-$ anion have small SO_2 capacities at a low pressure. The interactions between the $[NTf_2]^-$ anion and SO_2 are much weaker than those between the $[C_2OSO_3]^-$ anion and SO_2. The binding energies are calculated to be −10.6 kcal mol^{-1} for $[NTf_2]^-$−SO_2 and −17.4 kcal mol^{-1} for $[C_2OSO_3]^-$−SO_2, according to ref 45. This means, for ILs with the same cation, the ethyl sulfate ILs have better performance in SO_2 absorption as a result of enhanced intermolecular interactions of anion and SO_2, which is in good agreement with our experimental results.

In addition, no significant difference is observed for the chemical shifts in the ^{1}H NMR spectra (Figures S-10 and S-11 in the Supporting Information) of the ethyl sulfate ILs before and after the absorption of SO_2. This indicates that the interactions between IL and SO_2 are quite weak, no strong chemical interactions are involved, and no additional chemical bonds are formed. To confirm this result, FT-IR characterizations were carried out, which are graphically shown in Figure S-12. Still no remarkable change can be seen for $[C_2{}^2(C_1)_2(C_1)_2{}^3gu][C_2OSO_3]$. The intermolecular hydrogen-bonding interactions for the $[(C_2)_2{}^2(C_1)_2(C_1)_2{}^3gu][C_2OSO_3]$ and SO_2 system at the wavenumber of about 3500 cm^{-1} are observed, while additional shifts or new peaks are hardly found in the IR spectra. It should be the intrinsic intramolecular hydrogen-bonding interaction between the cation and anion of $[C_2{}^2(C_1)_2(C_1)_2{}^3gu][C_2OSO_3]$ that gives rise to the difference. The interaction enthalpies for IL−SO_2 shown in Table 2 also support that no chemical bond is formed, due to the relatively small values of Δ*H* for intermolecular interactions between IL and SO_2.

■ CONCLUSION

In this work, we successfully synthesized and applied two novel guanidinium ethyl sulfate ILs to capture SO_2. The low-cost ethyl sulfate ILs showed satisfactory abilities of absorption and regeneration. It is found that the amount of captured SO_2 (mole SO_2 per mole of IL) is in the order of $[(C_2)_2{}^2(C_1)_2(C_1)_2{}^3gu][C_2OSO_3]$ (3.93) > $[C_2{}^2(C_1)_2(C_1)_2{}^3gu]$-$[C_2OSO_3]$ (3.15) > $[(C_2)_2{}^2(C_1)_2(C_1)_2{}^3gu][NTf_2]$ (2.25) > $[C_2{}^2(C_1)_2(C_1)_2{}^3gu][NTf_2]$ (1.93) at 1 bar of SO_2 and 20 °C. The guanidinium ethyl sulfate ILs perform better than the imidazolium and pyridinium ethyl sulfate ILs under the same conditions. Moreover, the ILs captured 0.71, 1.08, 0.17, and 0.24 mol SO_2 per mole of IL at 0.1 bar of SO_2 in N_2 and at 20 °C by $[C_2{}^2(C_1)_2(C_1)_2{}^3gu][C_2OSO_3]$, $[(C_2)_2{}^2(C_1)_2(C_1)_2{}^3gu]$-$[C_2OSO_3]$, $[C_2{}^2(C_1)_2(C_1)_2{}^3gu][NTf_2]$ and $[(C_2)_2{}^2(C_1)_2(C_1)_2{}^3gu][NTf_2]$, respectively. On the basis of the quantum chemistry calculations, gas absorption is mainly governed by the interactions between the anion of IL and SO_2.

Table 2. Interaction Enthalpies (Δ*H*, kcal mol^{-1}) between ILs and SO_2

	Δ*H* (kcal mol^{-1})			
IL	+ $1SO_2$	+ $2SO_2$	+ $3SO_2$	+ $4SO_2$
$[C_2{}^2(C_1)_2(C_1)_2{}^3gu][C_2OSO_3]$	−8.1	−14.4	−23.1	−27.9
$[(C_2)_2{}^2(C_1)_2(C_1)_2{}^3gu][C_2OSO_3]$	−6.0	−16.1	−19.3	−27.8
$[C_2{}^2(C_1)_2(C_1)_2{}^3gu][NTf_2]$	−5.2	−11.6	−16.9	−20.5
$[(C_2)_2{}^2(C_1)_2(C_1)_2{}^3gu][NTf_2]$	−6.6	−11.9	−15.7	−20.1

DOI: 10.1021/acs.jpcb.5b00921

The hydrogen-bonding interaction of N−H···O in the penta-substituted guanidinium-based ILs prevents the interaction of ILs and SO_2. The nonbonded interactions between IL moieties and SO_2, along with interactions between SO_2 molecules through O═S···O were presented during the absorption process, which were supposed to be quite weak in accordance with ^1H NMR and FT-IR characterizations. In summary, theoretical and experimental researches have validated that the novel guanidinium ethyl sulfate ILs have the potential for SO_2 capture.

■ ASSOCIATED CONTENT

Ⓢ Supporting Information

Details for preparations of ILs, density and ^1H and ^{13}C NMR spectra of the guanidinium-based ILs, FT-IR spectra for ethyl sulfate ILs before and after SO_2 absorption, and Gaussian input file for quantum calculations. The Supporting Information is available free of charge on the ACS Publications website at DOI: 10.1021/acs.jpcb.5b00921.

■ AUTHOR INFORMATION

Corresponding Authors

*Telephone/Fax: +86-571-88981416. E-mail: wjjw@zju.edu.cn. (Y.G.).
*Telephone/Fax: +86-571-28008900. E-mail: hujunxie@gmail.com. (H.X.).
*Telephone/Fax: +86-571-88981416. E-mail: fwjun@zju.edu.cn. (W.F.).

Notes

The authors declare no competing financial interest.

■ ACKNOWLEDGMENTS

We are grateful for the financial support from the National Natural Science Foundation of China (Nos. 21273201 and J1210042).

■ REFERENCES

(1) Ma, X.; Kaneko, T.; Tashimo, T.; Yoshida, T.; Kato, K. Use of Limestone for SO_2 Removal from Flue Gas in the Semidry FGD Process with a Powder-Particle Spouted Bed. *Chem. Eng. Sci.* **2000**, *55*, 4643−4652.

(2) MacDowell, N.; Florin, N.; Buchard, A.; Hallett, J.; Galindo, A.; Jackson, G.; Adjiman, C. S.; Williams, C. K.; Shah, N.; Fennell, P. An Overview of CO_2 Capture Technologies. *Energy Environ. Sci.* **2010**, *3*, 1645−1669.

(3) Ramdin, M.; de Loos, T. W.; Vlugt, T. J. H. State-of-the-Art of CO_2 Capture with Ionic Liquids. *Ind. Eng. Chem. Res.* **2012**, *51*, 8149−8177.

(4) Cadena, C.; Anthony, J. L.; Shah, J. K.; Morrow, T. I.; Brennecke, J. F.; Maginn, E. J. Why Is CO_2 So Soluble in Imidazolium-Based Ionic Liquids? *J. Am. Chem. Soc.* **2004**, *126*, 5300−5308.

(5) Llovell, F.; Marcos, R. M.; MacDowell, N.; Vega, L. F. Modeling the Absorption of Weak Electrolytes and Acid Gases with Ionic Liquids Using the Soft-SAFT Approach. *J. Phys. Chem. B* **2012**, *116*, 7709−7718.

(6) Seo, S.; Simoni, L. D.; Ma, M.; De Silva, M. A.; Huang, Y.; Stadtherr, M. A.; Brennecke, J. F. Phase-Change Ionic Liquids for Postcombustion CO_2 Capture. *Energy Fuels* **2014**, *28*, 5968−5977.

(7) Aparicio, S.; Atilhan, M. On the Properties of CO_2 and Flue Gas at the Piperazinium-Based Ionic Liquids Interface: A Molecular Dynamics Study. *J. Phys. Chem. C* **2013**, *117*, 15061−15074.

(8) Karadas, F.; Atilhan, M.; Aparicio, S. Review on the Use of Ionic Liquids (ILs) as Alternative Fluids for CO_2 Capture and Natural Gas Sweetening. *Energy Fuels* **2010**, *24*, 5817−5828.

(9) Lei, Z. G.; Dai, C. N.; Chen, B. H. Gas Solubility in Ionic Liquids. *Chem. Rev.* **2014**, *114*, 1289−1326.

(10) Wang, C. M.; Zheng, J. J.; Cui, G. K.; Luo, X. Y.; Guo, Y.; Li, H. R. Highly Efficient SO_2 Capture Through Tuning the Interaction between Anion-Functionalized Ionic Liquids and SO_2. *Chem. Commun.* **2013**, *49*, 1166−1168.

(11) Morganti, J. D.; Hoher, K.; Ribeiro, M. C. C.; Ando, R. A.; Siqueira, L. J. A. Molecular Dynamics Simulations of Acidic Gases at Interface of Quaternary Ammonium Ionic Liquids. *J. Phys. Chem. C* **2014**, *118*, 22012−22020.

(12) Wu, W. Z.; Han, B. X.; Gao, H. X.; Liu, Z. M.; Jiang, T.; Huang, J. Desulfurization of Flue Gas: SO_2 Absorption by an Ionic Liquid. *Angew. Chem., Int. Ed.* **2004**, *43*, 2415−2417.

(13) Huang, J.; Riisager, A.; Berg, R. W.; Fehrmann, R. Tuning Ionic Liquids for High Gas Solubility snd Reversible Gas Sorption. *J. Mol. Catal. A: Chem.* **2008**, *279*, 170−176.

(14) Kohler, F.; Roth, D.; Kuhlmann, E.; Wasserscheid, P.; Haumann, M. Continuous Gas-Phase Desulfurisation Using Supported Ionic Liquid Phase (SILP) Materials. *Green Chem.* **2010**, *12*, 979−984.

(15) Murphy, L. J.; McPherson, A. M.; Robertson, K. N.; Clyburne, J. A. C. Ionic Lquids and Acid Gas Capture: Water and Oxygen as Confounding Factors. *Chem. Commun.* **2012**, *48*, 1227−1229.

(16) Huang, K.; Chen, Y. L.; Zhang, X. M.; Xia, S.; Wu, Y. T.; Hu, X. B. SO_2 Absorption in Acid Salt Ionic Liquids/Sulfolane Binary Mixtures: Experimental Study and Thermodynamic Analysis. *Chem. Eng. J.* **2014**, *237*, 478−486.

(17) Revelli, A. L.; Mutelet, F.; Jaubert, J. N. Reducing of Nitrous Oxide Emissions Using Ionic Liquids. *J. Phys. Chem. B* **2010**, *114*, 8199−8206.

(18) Shiflett, M. B.; Niehaus, A. M. S.; Yokozeki, A. Separation of N_2O and CO_2 Using Room-Temperature Ionic Liquid [bmim][BF_4]. *J. Phys. Chem. B* **2011**, *115*, 3478−3487.

(19) Ren, S. H.; Hou, Y. C.; Wu, W. Z.; Liu, Q. Y.; Xiao, Y. F.; Chen, X. T. Properties of Ionic Liquids Absorbing SO_2 and the Mechanism of the Absorption. *J. Phys. Chem. B* **2010**, *114*, 2175−2179.

(20) Gao, H. X.; Han, B. X.; Li, J. C.; Jiang, T.; Liu, Z. M.; Wu, W. Z.; Chang, Y. H.; Zhang, J. M. Preparation of Room-Temperature Ionic Liquids by Neutralization of 1,1,3,3-Tetramethylguanidine with Acids and their Use as Media for Mannich Reaction. *Synth. Commun.* **2004**, *34*, 3083−3089.

(21) Liang, S. G.; Zhou, Y. X.; Liu, H. Z.; Jiang, T.; Han, B. X. Immobilized 1,1,3,3-Tetramethylguanidine Ionic Liquids as the Catalyst for Synthesizing Propylene Glycol Methyl Ether. *Catal. Lett.* **2010**, *140*, 49−54.

(22) King, A. W. T.; Asikkala, J.; Mutikainen, I.; Järvi, P.; Kilpeläinen, I. Distillable Acid−Base Conjugate Ionic Liquids for Cellulose Dissolution and Processing. *Angew. Chem.* **2011**, *123*, 6425−6429.

(23) Lu, X. X.; Yue, L.; Hu, M. J.; Cao, Q.; Xu, L.; Guo, Y. S.; Hu, S. L.; Fang, W. J. Piperazinium-Based Ionic Liquids with Lactate Anion for Extractive Desulfurization of Fuels. *Energy Fuels* **2014**, *28*, 1774−1780.

(24) Fang, W. J.; Shao, D. B.; Lu, X. X.; Guo, Y. S.; Xu, L. Extraction of Aromatics from Hydrocarbon Fuels Using *N*−Alkyl Piperazinium-Based Ionic Liquids. *Energy Fuels* **2012**, *26*, 2154−2160.

(25) An, D.; Wu, L. B.; Li, B. G.; Zhu, S. P. Synthesis and SO_2 Absorption/Desorption Properties of Poly(1,1,3,3-tetramethylguanidine acrylate). *Macromolecules* **2007**, *40*, 3388−3393.

(26) Huang, J.; Riisager, A.; Wasserscheid, P.; Fehrmann, R. Reversible physical absorption of SO_2 by ionic liquids. *Chem. Commun.* **2006**, *38*, 4027−4029.

(27) Hong, S. Y.; Im, J.; Palgunadi, J.; Lee, S. D.; Lee, J. S.; Kim, H. S.; Cheong, M.; Jung, K. D. Ether-functionalized Ionic Liquids as Highly Efficient SO_2 Absorbents. *Energy Environ. Sci.* **2011**, *4*, 1802−1806.

(28) Lei, X. X.; Xu, Y. J.; Zhu, L.; Wang, X. H. Highly Efficient and Reversible CO_2 Capture through 1,1,3,3-Tetramethylguanidinium Imidazole Ionic Liquid. *RSC Adv.* **2014**, *4*, 7052−7057.

(29) Yuan, X. L.; Zhang, S. J.; Chen, Y. H.; Lu, X. M.; Dai, W. B.; Mori, R. Solubilities of Gases in 1,1,3,3-Tetramethylguanidium Lactate at Elevated Pressures. *J. Chem. Eng. Data* **2006**, *51*, 645−647.

(30) Wang, Y.; Wang, C. M.; Zhang, L. Q.; Li, H. R. Difference for SO_2 and CO_2 in TGML Ionic Liquids: a theoretical investigation. *Phys. Chem. Chem. Phys.* **2008**, *10*, 5976−5982.

(31) Tian, S. D.; Ren, S. H.; Hou, Y. C.; Wu, W. Z.; Peng, W. Densities, Viscosities and Excess Properties of Binary Mixtures of 1,1,3,3-Tetramethylguanidinium Lactate + Water at T = (303.15 to 328.15) K. *J. Chem. Eng. Data* **2013**, *58*, 1885−1892.

(32) Lu, X. X.; Cao, Q.; Wu, X.; Xie, H. J.; Lei, Q. F.; Fang, W. J. Conformational Isomerism Influence on the Properties of Piperazinium Bis(trifluoromethylsulfonyl)imide. *J. Phys. Chem. B* **2014**, *118*, 9085−9095.

(33) Beck, A. D. Density-functional Thermochemistry. III. The Role of Exact Exchange. *J. Chem. Phys.* **1993**, *98*, 5648−5652.

(34) Lee, C.; Yang, W.; Parr, R. G. Development of the Colle-Salvetti Correlation-Energy Formula into a Functional of the Electron Density. *Phys. Rev. B* **1988**, *37*, 785−789.

(35) Miehlich, B.; Savin, A.; Stoll, H. H.; Preuss, R. Results Obtained with the Correlation Energy Density Functionals of Becke and Lee, Yang and Parr. *Chem. Phys. Lett.* **1989**, *157*, 200−206.

(36) Gaussian 09, Revision A.1. Frisch, M. J.; Trucks, G. W.; Schlegel, H. B.; Scuseria, G. E.; Robb, M. A.; Cheeseman, J. R.; Scalmani, G.; Barone, V.; Mennucci, B.; Petersson, G. A.; et al. Gaussian, Inc.: Wallingford CT, 2009.

(37) Barrosse-Antle, L. E.; Hardacre, C.; Compton, R. G. SO_2 Saturation of the Room Temperature Ionic Liquid [C_2mim][NTf_2] Much Reduces the Activation Energy for Diffusion. *J. Phys. Chem. B* **2009**, *113*, 1007−1011.

(38) Ando, R. A.; Siqueira, L. J. A.; Bazito, F. C.; Torresi, R. M.; Santos, P. S. The Sulfur Dioxide−1-Butyl-3-Methylimidazolium Bromide Interaction: Drastic Changes in Structural and Physical Properties. *J. Phys. Chem. B* **2007**, *111*, 8717−8719.

(39) Cui, G. K.; Wang, C. M.; Zheng, J. J.; Guo, Y.; Luo, X. Y.; Li, H. R. Highly Efficient SO_2 Capture by Dual Functionalized Ionic Liquids through a Combination of Chemical and Physical Absorption. *Chem. Commun.* **2012**, *48*, 2633−2635.

(40) Holbrey, J. D.; Reichert, W. M.; Swatloski, R. P.; Broker, G. A.; Pitner, W. R.; Seddon, K. R.; Rogers, R. D. Efficient, Halide Free Synthesis of New, Low Cost Ionic Liquids: 1,3-Dialkylimidazolium Salts Containing Methyl- and Ethyl-Sulfate Anions. *Green Chem.* **2002**, *4*, 407−413.

(41) Luis, P.; Afonso, C. A. M.; Coelhoso, I. M.; Crespo, J.; Irabien, A. In *Proceedings of the 23rd European Symposium on Applied Thermodynamics*; 2008, ISBN: 2-905267-59-3.

(42) Luis, P.; Garea, A.; Irabien, A. Zero Solvent Emission Process for Sulfur Dioxide Recovery Using a Membrane Contactor and Ionic Liquids. *J. Membr. Sci.* **2009**, *330*, 80−89.

(43) Kim, I.; Svendsen, H. F. Heat of Absorption of Carbon Dioxide (CO_2) in Monoethanolamine (MEA) and 2-(Aminoethyl)-ethanolamine (AEEA) Solutions. *Ind. Eng. Chem. Res.* **2007**, *46*, 5803−5809.

(44) Shannon, M. S.; Irvin, A. C.; Liu, H.; Moon, J. D.; Hindman, M. S.; Turner, C. H.; Bara, J. E. Chemical and Physical Absorption of SO_2 by *N*−Functionalized Imidazoles: Experimental Results and Molecular-level Insight. *Ind. Eng. Chem. Res.* **2015**, *54*, 462−471.

(45) Damas, G. B.; Dias, A. B. A.; Costa, L. T. A Quantum Chemistry Study for Ionic Liquids Applied to Gas Capture and Separation. *J. Phys. Chem. B* **2014**, *118*, 9046−9064.

(46) Lourenço, T. C.; Coelho, M. F. C.; Ramalho, T. C.; van der Spoel, D.; Costa, L. T. Insights on the Solubility of CO_2 in 1-Ethyl-3-methylimidazolium Bis(trifluoromethylsulfonyl)imide from the Microscopic Point of View. *Environ. Sci. Technol.* **2013**, *47*, 7421−7429.

(47) Lin, H.; Freeman, B. D. Materials selection guidelines for membranes that remove CO_2 from gas mixtures. *J. Mol. Struct.* **2005**, *739*, 57−74.

(48) Shannon, M. S.; Tedstone, J. M.; Danielsen, S. P. O.; Hindman, M. S.; Irvin, A. C.; Bara, J. E. Free Volume as the Basis of Gas Solubility and Selectivity in Imidazolium-Based Ionic Liquids. *Ind. Eng. Chem. Res.* **2012**, *51*, 5565−5576.

(49) Li, P.; Paul, D. R.; Chung, T.-S. High Performance Membranes based on Ionic Liquid Polymers for CO_2 Separation from the Flue Gas. *Green Chem.* **2012**, *14*, 1052−1063.

(50) Fang, W.; Luo, Z.; Jiang, J. CO_2 Capture in Poly(Ionic Liquid) Membranes: Atomistic Insight into the Role of Anions. *Phys. Chem. Chem. Phys.* **2013**, *15*, 651−658.